

# Catalyst Parameters Determining Activity and Selectivity of Supported Gold Nanoparticles for the Aerobic Oxidation of Alcohols: The Molecular Reaction Mechanism

Alberto Abad, Avelino Corma,\* and Hermenegildo García\*[a]

**Abstract:** As previously reported for solventless reactions, gold nanoparticles supported on ceria are also excellent general heterogeneous catalysts for the aerobic oxidations of alcohols in organic solvents. Among organic solvents it was found that toluene is a convenient one. A systematic study on the influence of the particle size and gold content on the support has established that the activity correlates linear-

ly with the total number of external gold atoms, and with the surface coverage of the support. Amongst catalysts with different supports, but similar gold particle size and content, gold on ceria exhibits the highest activity. By means

of a kinetic study (influence of  $\sigma^+$  parameter, kinetic isotopic effect, temperature, alcohol concentration and oxygen pressure) a mechanistic proposal consisting of the formation of metal–alcoholate,  $\beta$ -hydride shift from carbon to metal and M–H oxidation has been proposed that explains all experimental results.

**Keywords:** alcohols • gold • heterogeneous catalysis • nanoparticles • oxidation

## Introduction

Homogeneous and heterogeneous gold nanoparticles show interesting activity for a large number of reactions involving alkynes,<sup>[1–6]</sup> alkenes,<sup>[7–12]</sup> selective hydrogenations,<sup>[13–18]</sup> and oxidations<sup>[19–24]</sup> among others.<sup>[25]</sup>

Among the different reactions, selective oxidation of alcohols to carbonylic compounds is one of the most important transformations in organic chemistry. It is the final goal for solid catalysts to be able to perform this reaction with air at atmospheric pressure and low temperature, as well as to replace current stoichiometric alcohol oxidation by a general catalyst that is selective for any hydroxyl group. In response to this goal, various gold,<sup>[26–27]</sup> palladium,<sup>[28]</sup> and gold/palladium<sup>[29]</sup> catalysts have given good results. Among these noble metals, gold, though less active than Pd or Au/Pd for some alcohols, is of more general use and exhibits higher selectivity than either Pd or Au/Pd.<sup>[30–31]</sup> Owing to the interesting

catalytic properties of Au for selective oxidations, we have carried out a detailed mechanistic study that addresses the influence of the gold nanoparticle size, nature of the support and influence of catalyst preparation procedure, to establish a detailed reaction mechanism that can help to design a new generation of more active gold catalysts for the aerobic oxidation of alcohols.

## Results and Discussion

The current research field of gold catalysis has been developed following the seminal contribution of Haruta, who (for low temperature CO oxidation) showed that small gold nanoparticles exhibited a high catalytic activity and that this catalytic activity was a function of the gold particle size.<sup>[32]</sup> Following this work, it would be of interest to ascertain whether or not the same relationship between size and activity also takes place in the catalytic oxidation of alcohols. Aimed at determining the influence of the nanoparticles size on gold catalytic activity for alcohol oxidation we have prepared a series of six different samples of gold supported on titania, in which the average particle size has been varied in the range from 5 to 25 nm. For this study, titanium dioxide (P-25 Degussa) was considered a suitable support, as on one hand it makes the transmission electron microscopy study of the particle size easier (average particle size 35 nm,

[a] Dr. A. Abad, Prof. Dr. A. Corma, Prof. Dr. H. García  
Instituto de Tecnología Química CSIC-UPV  
Universidad Politécnica de Valencia  
Av. De los Naranjos s/n, 46022 Valencia (Spain)  
Fax: (+34)963-877-809  
E-mail: acorma@itq.upv.es  
hgarcia@qim.upv.es

P-25 TiO<sub>2</sub>) and on the other hand, Au–TiO<sub>2</sub> exhibits high catalytic activity for alcohol oxidation reactions.<sup>[33–35]</sup>

In general, adjusting the average gold nanoparticle size in prepared samples of Au–TiO<sub>2</sub> can be achieved by varying, in a controlled way, any of the experimental parameters during the deposition–precipitation general procedure. Specifically, the pH (in the range between pH 9 and 4) at which the precipitation is conducted is a key factor determining the size of the resultant supported nanoparticles. Other parameters such as calcination temperature and the ratio between support and gold are interrelated and also have a definitive effect on the particle size.<sup>[36–37]</sup> The particle size distribution was determined by transmission electron microscopy (TEM) and ranged from 5–25 nm. The catalytic activity of these samples was tested for the aerobic oxidation of cinnamyl alcohol, this alcohol was selected as model compound because it allows to determine not only differences in activity, but also differences in chemoselectivity.

Figure 1 plots the turnover frequency (TOF) of cinnamaldehyde formation versus the average particle size. It can be seen these that the activity of the catalysts decreases exponentially with the increase in particle size. It has to be pointed out that the only product detected in all cases was cinnamaldehyde and that the selectivity is independent on gold particle size.

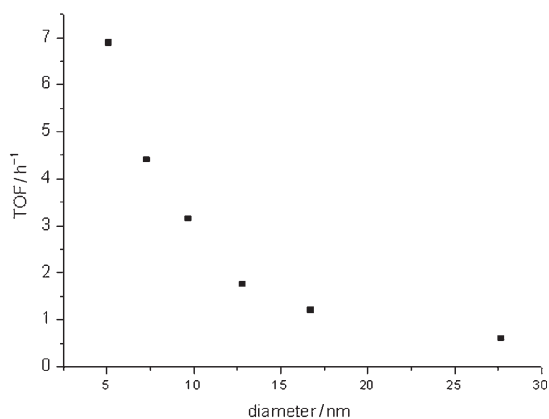


Figure 1. TOF values for the oxidation of cinnamyl alcohol given as the ratio of moles of cinnamaldehyde per mole Au per hour (measured at  $t = 20$  min) versus the gold mean particle diameter in Au–TiO<sub>2</sub> catalysts. Reaction conditions: cinnamyl alcohol (1 mmol), toluene (5 mL), catalyst (5 mol % Au), air (1 atm), 90 °C.

In an attempt to rationalize the experimental relationship between TOF and gold particle size we proceeded to estimate the number of external surface atoms for each catalyst on the basis of the mean particle size. According to the TEM images, which reveal that the shape of gold nanoparticles is predominantly cubic, we assume that the titania supported gold nanoparticles can be modelled as a *fcc* crystal lattice. Although this simple model represents an oversimplification, it allows the estimation of the number of particle gold atoms ( $N_T$ ) according to Equation (1) in which  $\langle d \rangle$  cor-

responds to the mean diameter of gold particles as determined experimentally by TEM and  $d_{at}$  is the atomic diameter of gold (0.288 nm). Considering that in the *fcc* crystal one atom is surrounded by twelve others assuming a full shell close packing model and  $N_T$  is related to the number of shells ( $m$ ) [Eq. (2)] then the number of external atoms can be estimated as indicated by Equation (3).<sup>[38–39]</sup>

$$N_T = \frac{(10m^3 - 15m^2 + 11m - 3)}{3} \quad (1)$$

$$\langle d \rangle = 1.105 \times d_{at} \times N_T^{1/3} \quad (2)$$

$$N_s = 10m^2 - 20m + 12 \quad (3)$$

When the catalytic data are plotted versus the total number of external gold atoms ( $N_s$ ) instead of the average particle size, a linear plot is obtained (Figure 2). This indi-

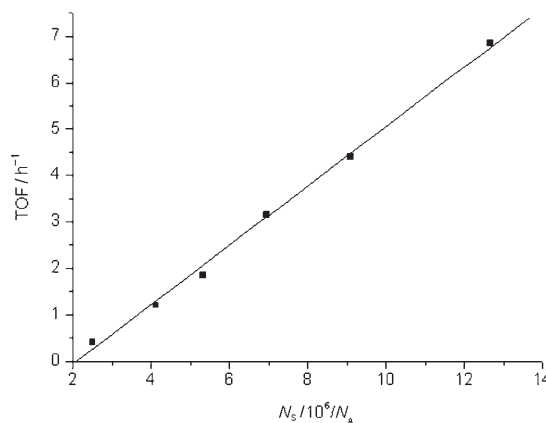


Figure 2. TOF values for the oxidation of cinnamyl alcohol versus the number of external gold atoms ( $N_s$ ) present in the amount of Au–TiO<sub>2</sub> catalysts with different particle size used in the aerobic oxidation reactions (see Figure 1 for reaction conditions,  $N_A$ : Avogadro's number).  $r^2 = 0.99$ , slope = 0.663.

cates that the intrinsic activity per external gold atom is independent of the particle size. A similar correlation has also found for the aerobic oxidation of glucose by *naked* gold nanoparticles.<sup>[26]</sup> Analysis of previous results, leads us to conclude that to optimize the catalytic activity of gold for oxidations the metal dispersion should be increased, as gold particle size has no effect on selectivity, at least, for the reactant studied here.

**Influence of the nature of the support on the catalytic activity of gold nanoparticles:** There is some controversy in the literature about the role and the influence of the support on the activity of supported gold nanoparticles. Rossi and co-workers reported that *naked* gold nanoparticles can be highly active for the aerobic oxidation of glucose and other polyalcohols, the role of activated carbon as support is to stabilize the nanoparticles against aggregation. On the other

hand, we have reported a synergic effect between gold and the ceria nanoparticles (npCeO<sub>2</sub>), the nanometric size of the support boosts the catalytic activity. To discuss the potential role of the support for gold catalyzed oxidations, we have proceeded to prepare a series of supported gold catalysts with the same gold content (1.5–2 wt%) and particle size (3–4 nm), but with a variety of supports. It is clear that, owing to inherent experimental limitations, this series of catalysts has some minor variations in gold content and size distribution. In spite of these variations, the series can be considered homogeneous enough to prove or disprove the influence of the support. The results shown in Figure 3 clear-

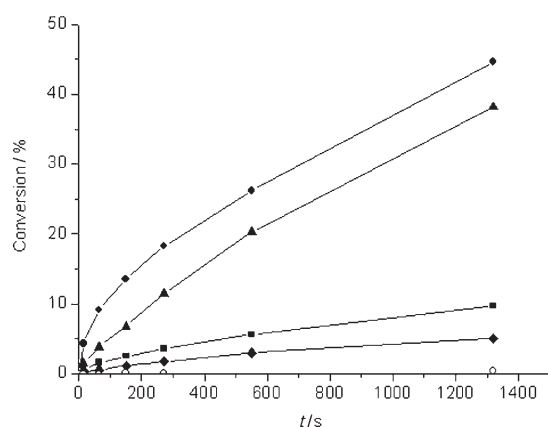


Figure 3. The time-conversion plot for cinnamyl alcohol oxidation with different gold catalysts. Reaction conditions: cinnamyl alcohol (1 mmol), toluene (5 mL), catalyst (0.2 mol% Au), air (1 atm), 90 °C. ●: 1.8 wt% Au/npCeO<sub>2</sub> (*d* = 4.4 nm); ▲: 2 wt% Au/CeO<sub>2</sub> (*d* = 4.2 nm); ■: 1.5 wt% Au–TiO<sub>2</sub> (*d* = 3.6 nm); ◆: 2 wt% Au/C (*d* = 3.6 nm); ○: without catalyst.

ly show that catalyst activity is strongly dependent on the nature of the support (gold supported on ceria (Au/npCeO<sub>2</sub>) the most and gold supported on activated carbon (Au/C) the least active).

The data obtained indicate the suitability of ceria, particularly in the form of nanoparticles, as compared to titania and carbon as supports. In a first approximation, we propose that lattice oxygen vacancies, which are more abundant in nanoparticulated ceria,<sup>[40]</sup> can be the factor that enhances the activity of the support by favouring interaction and physisorption of molecular oxygen. We will come back to this point later.

It is also worth commenting on the low catalytic activity of Au/C for the aerobic oxidation of cinnamyl alcohol in toluene and in the absence of base. In contrast, it has been reported that Au/C is highly active for the aerobic oxidation of polyols in basic aqueous solutions. Under these conditions colloidal gold is equally active also.<sup>[6]</sup> However, in the absence of base, as it is here, colloidal gold is catalytically poorly active.

**Optimization of preparation procedure and gold content for Au/npCeO<sub>2</sub>:** As Au/npCeO<sub>2</sub> is a highly active catalyst for the aerobic alcohol oxidation. We have optimized the preparation procedure and gold content, in order to produce the most active catalyst possible. In this context, one issue that has attracted attention in the literature is whether or not the preparation procedure influences the catalytic activity of supported gold nanoparticles or it is just a way of achieving different metal dispersion,<sup>[41]</sup> to address specifically this point and considering that reduction by thermal treatment and reduction by using an alcohol as reducing reagent are the two most widely used reduction procedures, we have prepared a series of six samples in which gold has always been deposited on nanocrystalline ceria by the deposition–precipitation method of a tetrachloroauric acid solution at pH 10 and after that the activation procedure has been varied. Figure 4 shows the samples prepared as well as the

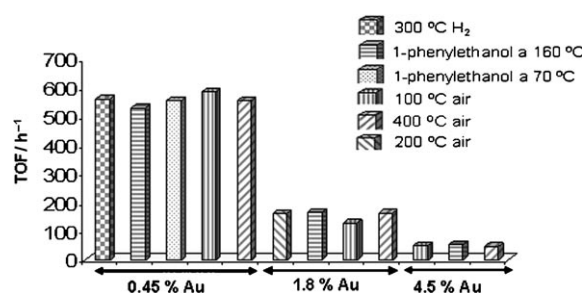


Figure 4. TOF values for the oxidation of cinnamyl alcohol given as the ratio of moles of cinnamaldehyde per mole Au per hour (measured at *t* = 20 min) for Au/npCeO<sub>2</sub> synthesized with different gold loadings and different reducing pretreatments. Reaction conditions: cinnamyl alcohol (1 mmol), toluene (5 mL), catalyst (0.2 mol% Au), air (1 atm), 90 °C.

TOF values measured for these samples for the aerobic oxidation of cinnamyl alcohol. Two samples were prepared by reducing gold with benzyl alcohol at 70 or 160 °C. It was expected that higher reduction temperatures would produce the gold nanoparticles more quickly and consequently, more active gold nanoparticles could be generated. Analogously the samples were also reduced by thermal calcination at 100, 200 and 400 °C in air and in one case at 400 °C under hydrogen. It was expected that thermal treatment at high temperatures could produce particle agglomeration, whereas lower temperatures and hydrogen atmosphere could lead to partial reduction with a larger population of positive gold atoms. As it can be seen in Figure 4, the different metal reduction treatments studied here have no influence on the final catalytic activity, the samples giving a reproducible and fairly constant TOF value, regardless of the reduction procedure.

In contrast, the gold content of the support plays an important role determining the catalytic activity. Samples differing in the gold/support mass ratio were prepared by deposition–precipitation (pH 10) of HAuCl<sub>4</sub> and low temperature reduction with hydrogen. The most active catalysts for

the oxidation of cinnamyl alcohol are those that contain the lowest gold percentage on the support.

To rationalize the remarkable influence of the gold loading on ceria nanoparticles, we carried out a study by means of TEM of the particle size distribution for three representative samples. The results are included in Table 1 and they

Table 1. Gold nanoparticle size and TOF values for the oxidation of cinnamyl alcohol catalyzed by a series of Au/npCeO<sub>2</sub> catalysts with different gold content.<sup>[a]</sup>

Au [%]	$\langle d \rangle$ [nm]	TOF [h <sup>-1</sup> ] <sup>[b]</sup>
0.44	4.9	530
1.80	4.4	167
4.45	9.2	54

[a] Reaction conditions: cinnamyl alcohol (1 mmol), toluene (5 mL), catalyst (0.2 mol% Au), air (1 atm), 90°C. The Au/npCeO<sub>2</sub> samples have been reduced with 1-phenylethanol at 160°C. [b] TOF values measured at  $t=20$  min.

show that although for the sample with the highest gold content, the average particle size distribution is significantly larger, for the samples with 0.44 and 1.8 wt% gold on npCeO<sub>2</sub> the size distribution is almost coincident. Nevertheless, in spite of the same particle size, the sample with 0.44 wt% of gold is significantly more active than the sample with 1.8 wt% of gold. A reasonable explanation to justify the large differences in activity between two gold catalysts prepared following the same method and exhibiting the same particle size distribution, but different gold content on the support relies on accepting that the free surface of ceria nanoparticles plays a role in catalysis. If the free ceria surface is covered by gold to a significant extent then the catalytic activity is reduced. In other words, both gold and ceria surfaces are required in the reaction mechanism. As discussed below, the reaction mechanism on the ceria surface cooperates with the catalysis by interacting with molecular oxygen. By means of oxygen physisorption, nanocrystalline ceria acts as an oxygen pump ensuring the oxidation of metal hydrides into water. This function requires that free ceria surface is present in the system.

**General synthetic utility of Au/npCeO<sub>2</sub> for the aerobic oxidation of alcohols in organic solvents:** Up to now most of the work on the aerobic alcohol oxidation by supported gold nanoparticles has been carried out under solvent-less conditions or in aqueous solutions.<sup>[18]</sup> However, most of the primary alcohols are oxidized to the corresponding carboxylates in aqueous basic solution and there are also certain circumstances in which an organic solvent is needed, owing to the limited availability of the alcohol or its high melting point. In these cases the use of an organic solvent is necessary to carry out the reaction properly. We have used a series of organic solvents that, in contrast with most oxidations in aqueous media, allow the reaction to proceed without base. A literature survey shows that most gold metal catalysts are inactive when the oxidation is carried out in the absence of a base.<sup>[42]</sup> Figure 5 shows the time-conversion plot for the

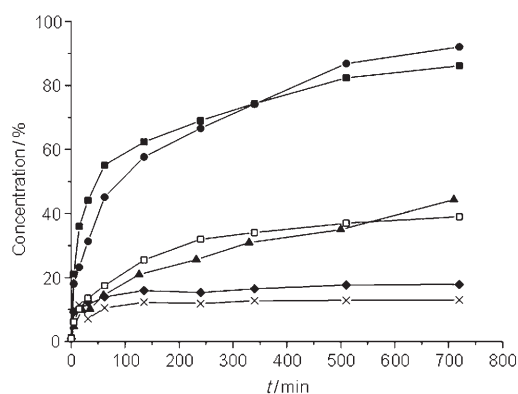


Figure 5. The time-conversion plot for benzyl alcohol oxidation with Au/npCeO<sub>2</sub> (0.44 wt% Au) in different solvents: toluene (●), trifluorotoluene (■), ethyl acetate (▲), Bmim[PF<sub>6</sub>] (□), acetonitrile (◆), ethanol (×). Reaction conditions: benzyl alcohol (1 mmol), solvent (5 mL), catalyst (0.2 mol% Au), air (1 atm), 75°C.

aerobic oxidation of benzyl alcohol catalyzed by Au/npCeO<sub>2</sub> in different solvents (toluene and trifluorotoluene are shown to be the most appropriate solvents). Moreover, after the reaction the catalyst can be recovered and reused. In contrast, if acetonitrile and ethanol are used as solvents, the activity of Au/npCeO<sub>2</sub> is significantly lower and the catalyst deactivates very quickly. This could be a result of the leaching of gold when using more polar solvents. Indeed, the chemical analysis of the used catalyst, after filtration and washing with clean solvent indicates a  $\approx 10$  wt% loss of the gold that was initially present. This is also the case if 1-butyl-3-methylimidazolium hexafluorophosphate ionic liquid (Bmim[PF<sub>6</sub>]) is used. Therefore, although the use of ionic liquids in combination with noble metal nanoparticles has been frequently reported in the literature as a convenient catalytic system,<sup>[43–45]</sup> the results obtained in our case were clearly unsatisfactory.

By using toluene as solvent, we have performed the aerobic oxidation of a wide range of alcohols in the presence of Au/npCeO<sub>2</sub> with the aim of showing the generality and limitations of Au/npCeO<sub>2</sub>, particularly in those cases in which heteroatoms or other functional groups are present. It is important to remark that oxidations were carried out with air instead of pure oxygen, making the process safer and more amenable from a practical point of view. Table 2 summarizes the reaction conditions, the products obtained and the corresponding selectivities.

Benzylic alcohols, either primary or secondary, were converted to the corresponding benzylic aldehydes or ketones in quantitative yields (see Table 2). The presence of substituents on the aromatic ring such as NO<sub>2</sub>-, Cl- or CH<sub>3</sub>O-, influenced the reaction rate, but did not affect the selectivity of the process or the resultant deactivation of the gold catalysts.

We reported previously that for oxidations carried out in the absence of solvent,<sup>[27]</sup> the catalyst Au/npCeO<sub>2</sub> was also found highly selective for the oxidation of organic substrates containing C=C double bonds. Thus, primary and secondary

Table 2. Oxidation of various alcohols with atmospheric air catalyzed by Au/npCeO<sub>2</sub>.

Substrate	<i>t</i> [h]	Conversion [%] <sup>[a]</sup>	Product	Selectivity [%] <sup>[a]</sup>
benzyl alcohol <sup>[b]</sup>	2	98	benzaldehyde	99
4-methylbenzyl alcohol <sup>[b]</sup>	2	> 99	4-methylbenzaldehyde	> 99
4-methoxybenzyl alcohol <sup>[b]</sup>	2	> 99	4-methoxybenzaldehyde	> 99
4-chlorobenzyl alcohol <sup>[b]</sup>	8	99	4-chlorobenzaldehyde	> 99
4-nitrobenzyl alcohol <sup>[b]</sup>	24	> 99	4-nitrobenzaldehyde	96
1-phenylethanol <sup>[b]</sup>	2	98	acetophenone	97
cyclopropylphenylmethanol <sup>[b]</sup>	2	> 99	cyclopropyl phenyl ketone	> 99
2-octanol <sup>[c]</sup>	3	97	2-octanone	> 99
2-adamantanol <sup>[c]</sup>	2	> 99	2-adamantanone	> 99
(-)-borneol <sup>[d]</sup>	24	91	camphor	98
2-octen-1-ol <sup>[d]</sup>	2	90	2-octenal	91
3-octen-2-ol <sup>[b]</sup>	20	96	3-octen-2-one	94
1-octen-3-ol <sup>[b]</sup>	6	> 99	1-octen-3-one	90
<i>trans</i> -carveol <sup>[b]</sup>	20	88	carvone	99
1-octanol <sup>[e]</sup>	4	47	octanal	91
<i>meso</i> -hydrobenzoin <sup>[b]</sup>	2	98	benzaldehyde	62
1,2-benzenedimethanol <sup>[b]</sup>	20	> 99	phthalide	98
<i>cis</i> -1,2-cyclohexanedio <sup>[c]</sup>	20	10	1,2-cyclohexanedione	42
2-thiophenemethanol <sup>[f]</sup>	7	96	2-thiophenecarboxaldehyde	54
2-furfuryl alcohol <sup>[f]</sup>	20	99	2-furfural	50
2-pyridinemethanol <sup>[d]</sup>	7	99	2-pyridinecarboxaldehyde	65

[a] Conversion and selectivity were determined by GC-MS or HPLC-MS. [b] Substrate (1 mmol), toluene (5 mL), Au/npCeO<sub>2</sub> 0.45 % (0.2 mol %), 90 °C, atmospheric air as oxidant. [c] Same as [b], but Au/npCeO<sub>2</sub> 1.8 wt % (0.4 mol %). [d] Same as [b], but Au/npCeO<sub>2</sub> 1.8 % (1.6 mol %). [e] Same as [b], but Au/npCeO<sub>2</sub> 4.5 % (1.6 mol %). [f] Same as [b], but Au/npCeO<sub>2</sub> 1.8 % (3.2 mol %).

$\alpha,\beta$ -unsaturated alcohols were oxidized to the corresponding unsaturated aldehydes or ketones without observing intramolecular hydrogen transfer, *cis,trans*-isomerization, epoxidation or polymerization of the C=C bond.

Likewise, Au/npCeO<sub>2</sub> can also oxidize secondary alcohols, either cyclic or aliphatic, with high yields. Sterically encumbered alcohols such as 2-adamantanol and borneol were equally oxidized to the corresponding ketones, although in these cases larger molar percentages of gold were necessary (see footnotes [c] and [d] in Table 2) to achieve high yields.

Primary aliphatic alcohols are selectively oxidized to the corresponding aliphatic aldehydes up to moderate conversions (see Table 2 for 1-octanol). When conversion increases, selectivity towards the aldehyde decreases significantly, owing to overoxidation of the aldehyde to the corresponding carboxylic acid. This selectivity problem can be alleviated by adding Au/npCeO<sub>2</sub> catalyst with a higher gold content, even though the initial reaction rate of this highly loaded catalyst is somewhat lower. To illustrate this point, Figure 6 shows the time-conversion plot for the aerobic oxidation of 1-octanol using two different Au/npCeO<sub>2</sub> catalysts. The graph in Figure 6 shows that a 90 % selectivity can be achieved at conversions lower than 45 % for Au/npCeO<sub>2</sub> 4.5 wt %. However, as the reaction progresses, selectivity decreases remarkably, owing to the formation of octanoic acid, although small amounts of heptanal and heptanoic acid (overall yield < 5 %) were also observed. The negative side effect of this overoxidation is that the presence of carboxylic acids in organic solvents in the absence of base causes strong deactivation of the gold catalysts. This poisoning in organic solvents is in contrast to our previous observation in strongly basic aqueous solution in which high selectivity towards octanoic acid at high conversions was achieved. Thus,

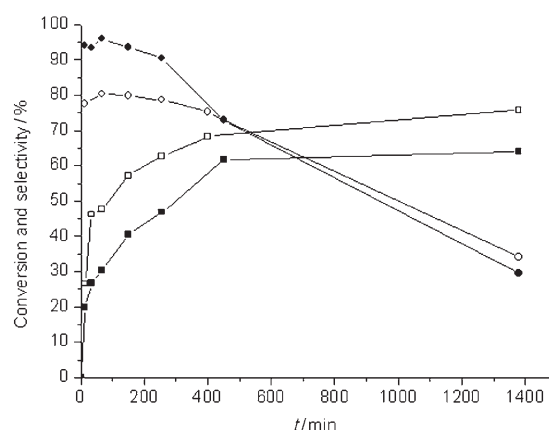


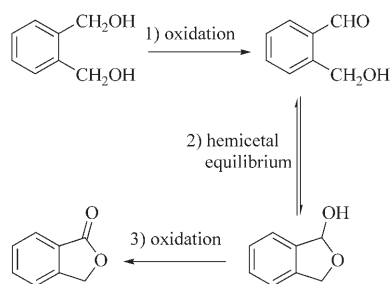
Figure 6. Temporal evolution of conversion and selectivity for the oxidation of 1-octanol to 1-octanal with Au/npCeO<sub>2</sub> in toluene. Reaction conditions: 1-octanol (1 mmol), toluene (5 mL), catalyst (1.6 mol % Au), air (1 atm), 90 °C. ●: selectivity with 4.5 wt % Au/npCeO<sub>2</sub>; ■: conversion with 4.5 wt % Au/npCeO<sub>2</sub>; ○: selectivity with 1.8 wt % Au/npCeO<sub>2</sub>; □: conversion with 1.8 wt % Au/npCeO<sub>2</sub>.

the highest yield for octanal in the aerobic oxidation in toluene was 45 %. The Au/npCeO<sub>2</sub> catalyst, even in those cases in which significant amounts of carboxylic acids are formed, was conveniently reactivated by washing with acetonitrile followed by 0.5 M NaOH aqueous solution and drying, recovering the same activity and selectivity characteristic of the fresh Au/npCeO<sub>2</sub> catalyst.

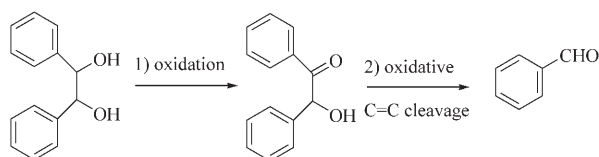
Another issue from Table 2 that deserves special comment, is the remarkable activity of Au/npCeO<sub>2</sub> to promote the aerobic oxidation of alcohols containing heteroatoms such as oxygen, sulphur and nitrogen heterocycles. Particularly relevant is the activity if nitrogen and sulphur atoms

are present, as it is known that these elements can strongly bind to gold nanoparticles. The temporal profile of these oxidations shows that formation of the corresponding aldehyde is very selective at low conversions, selectivity decreasing with conversion. Product analysis showed that the selectivity decrease is a result of the overoxidation of aldehydes to carboxylic acids and also to the formation of an array of by-products derived from the oxidative decomposition of the heterocycle.

The Au/npCeO<sub>2</sub> catalyst was also tested for the aerobic oxidation of *vic*-diols. In this way, the reaction of 1,2-benzenedimethanol gave rise to the formation of the corresponding isobenzofuranone in quantitative yields. The formation of this lactone can be explained by a route involving initial oxidation of one methanol group to aldehyde followed by acetalisation and a second oxidation of the hemiacetal. Scheme 1 shows the proposed route to explain the formation of the aromatic lactone. On the other hand, hydrobenzoin undergoes oxidative C=C cleavage to form benzaldehyde as the main product (Scheme 2).



Scheme 1. The proposed intermediates for the formation of the corresponding lactone by oxidation of 1,2-benzenedimethanol.



Scheme 2. The proposed intermediate for the formation of benzaldehyde by oxidation of *meso*-hydrobenzoin.

Finally, we have also studied the reuse of the 0.45 wt% Au/npCeO<sub>2</sub> catalyst by using the aerobic oxidation of benzylic alcohol as test reaction. The results are presented in Figure 7. Upon reuse, the catalyst maintains the initial activity throughout the six consecutive runs assayed, without appreciable decay in the selectivity. As for the solvent-less conditions, it is important to remark that the Au/npCeO<sub>2</sub> catalyst has to be exhaustively washed with a 0.5 M aqueous NaOH solution, to maintain the activity through the consecutive runs. Apparently basic washings are effective because they get rid of the carboxylic acids strongly adsorbed on the catalyst surface that ultimately lead to catalyst poisoning. In fact, if reuse is attempted without basic washings, the cata-

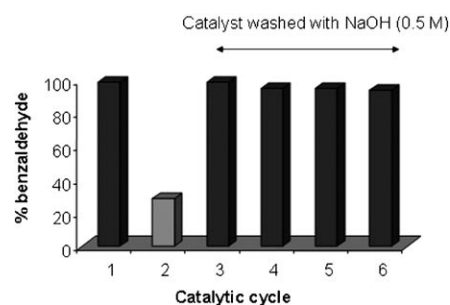


Figure 7. Evolution of the yield of benzaldehyde during six consecutive catalytic uses for the oxidation of benzyl alcohol with Au/npCeO<sub>2</sub> (0.44 wt%) catalyst.

lytic activity of Au/npCeO<sub>2</sub> is dramatically reduced (see Figure 7). However, even this deactivated catalyst recovers the activity of fresh Au/npCeO<sub>2</sub> after NaOH washings.

One important issue when working with heterogeneous systems is to determine whether or not leaching of gold occurs during the course of the reaction. To address this point we performed the aerobic oxidation of benzylic alcohols in toluene at 90 °C and the solid was removed by hot filtration after 30 minutes. The resultant clear solution was heated at 90 °C for longer periods without observing any conversion under these conditions. Furthermore the solution was analyzed by atomic absorption spectroscopy, whereby the presence of gold could not be detected.

On the other hand the basic aqueous solutions employed for the washings of Au/npCeO<sub>2</sub> before reuse were also analyzed for the presence of gold. In fact, gold was detected in all these washings and its quantification indicates that following the experimental procedure for catalyst reactivation produces around 2% depletion of the initial amount of gold present of ceria. This analysis of the washing waters was also performed for each of the runs corresponding to the consecutive reuses of the Au/npCeO<sub>2</sub> catalyst for the aerobic oxidation of benzylic alcohol, observing consistently the presence of gold in identical concentration. Additionally the gold content on Au/npCeO<sub>2</sub> after six consecutive catalytic runs was also analyzed by X-ray fluorescence spectroscopy. The results indicate a certain decrease in the gold loading that was estimated in about 10% of the initial loading. The total gold depletion on Au/npCeO<sub>2</sub> after six uses is consistent with the analysis of the washing waters and indicates that gold leaching only occurs during the washings with NaOH.

### Kinetic parameters and mechanistic aspects

*Mechanistic experiments:* Concerning the reaction mechanism for the aerobic oxidation of alcohols catalyzed by gold we addressed in the first place the possibility that the reaction mechanism involved carbon-centred free radicals as reaction intermediates. This possibility was however disregarded because the presence of unsaturated products arising from the ring aperture was not detected during the oxida-

tion of cyclopropyl phenyl carbinol to the corresponding cyclopropyl phenyl ketone. Also there was no influence on the initial reaction rate and conversion by the presence of radical trapping compounds such as 2,2,6,6-tetramethylpiperidine-N-Oxide (TEMPO) and hydroquinone. At this point a second reaction mechanism was considered that could proceed by the intermediacy of positively charged species. To check this, we have studied the influence of the ring substituents with various electron donating/electron withdrawing ability in the *para*-position of benzylic alcohol, on reaction rate. Figure 8 shows the plot of the logarithm of the

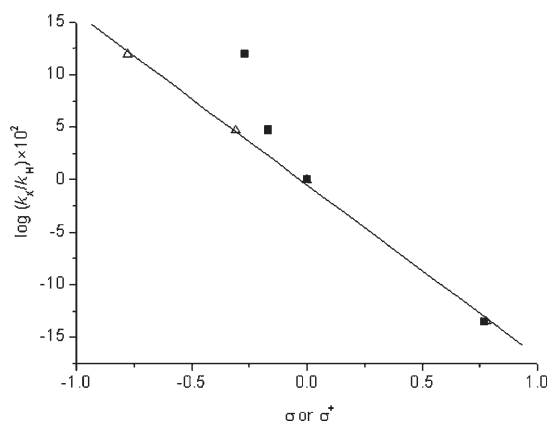


Figure 8. Hammett plots for competitive oxidation of benzyl alcohol and *p*-substituted benzyl alcohols. ■:  $\log(k_x/k_H)$  versus  $\sigma$ ;  $\Delta$ :  $\log(k_x/k_H)$  versus  $\sigma^+$ . Reaction conditions: benzyl alcohol (1 mmol), 0.44 wt % Au/npCeO<sub>2</sub> (0.2 mol %), toluene (5 mL), 90 °C, air (1 atm).

rate constants plotted against  $\sigma$  and  $\sigma^+$  that represents the Hammett and Brown–Okamoto parameters for each substituent. As it can be seen in this figure there is a reasonable linearity between  $\log(k_x/k_H)$  and the  $\sigma^+$  parameters giving a negative slope ( $\rho = -0.163$ ,  $r^2 = 0.99$ ).

The low negative  $\rho$  value indicates that the reaction is favoured by the presence in the *para*-position of electron donating groups. Also the fact that the  $\log k_x/k_H$  fits better with  $\sigma^+$  values indicates that the reaction intermediate should have a carbocationic character on the benzylic carbon.

On the other hand a primary isotopic effect was observed when comparing the reaction rates of *p*-methylbenzyl and  $\alpha$ -deutero-*p*-methylbenzyl alcohols. Figure 9 shows the influence of the monodeuteration in the benzylic position, on the time conversion plot for the initial reaction period. From these plots,  $k_H/k_D$  ratio was estimated to range from 1.7–2.0 for temperatures between 60–100 °C. These values (particularly considering that they were obtained for the  $\alpha$ -monodeuterated derivative) indicate that a remarkable isotopic effect is taking place, supporting the idea that a C–H bond breaking occurs in the rate-determining step of the reaction mechanism.

To reconcile the linearity between  $\log(k_x/k_H)$  versus  $\sigma^+$ , that indicates development of positive charge in the benzylic position, with the observation of a large kinetic isotopic

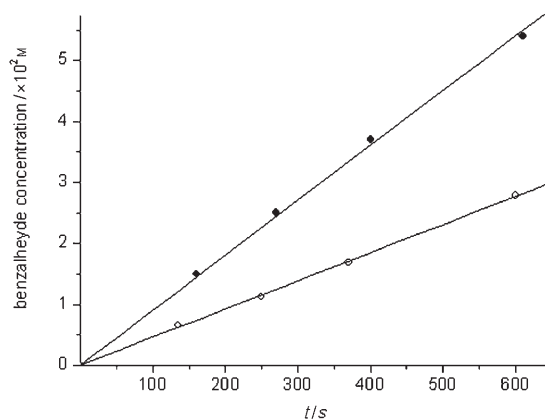
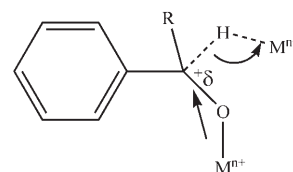


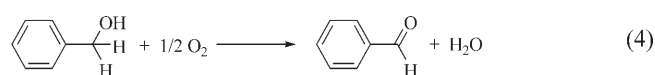
Figure 9. Isotopic effect in the aerobic oxidation of *p*-methylbenzyl alcohol (●) and  $\alpha$ -deutero-*p*-methylbenzyl alcohol (○) using 0.44 wt % Au/npCeO<sub>2</sub> as catalyst. Reaction conditions: benzylic alcohol (1 mmol), Au/npCeO<sub>2</sub> (0.2 mol %), toluene (5 mL), 81 °C and atmospheric air as oxidant.

effect. We propose that the rupture of the benzylic C–H bond progresses faster than the formation of the C=O and that the C–OH develops a partial positive charge in the transition state (see Scheme 3).



Scheme 3. The proposed transition state in the aerobic oxidation of alcohols with gold catalysts.

**Macroscopic kinetic work:** Firstly we have experimentally determined the stoichiometry of the global oxidation reaction occurring on Au/CeO<sub>2</sub>. To address this issue we measured the oxygen consumption for the oxidation of benzylic alcohol at 90 °C. Figure 10 shows a correlation between oxygen consumption and the number of moles of benzaldehyde formed concomitantly. This plot strongly supports that the moles of benzaldehyde formed are double than the moles of oxygen consumed, in agreement with the reaction stoichiometry indicated in Equation (4).



For the determination of the kinetic rate expression, the influence of reactant concentration has been studied. Thus, a series of benzylic alcohol oxidations were carried out at constant concentration, but varying the oxygen pressure (Figure 11). By measuring the initial reaction rate ( $r_0$ ), we

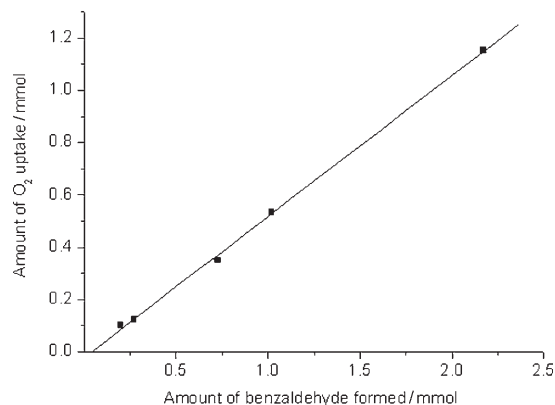


Figure 10. Relationship between amount of benzaldehyde produced and  $O_2$  uptake for the oxidation of benzyl alcohol with molecular oxygen catalyzed by 0.44 wt% Au/npCeO<sub>2</sub>. Reaction conditions: benzyl alcohol (3 mmol), 0.44 wt% Au/npCeO<sub>2</sub> (0.2 mol%), toluene (15 mL), 90 °C,  $O_2$  (air, 1 atm). Slope ( $O_2$  uptake/benzaldehyde formed) = 0.54 ( $r^2 = 0.99$ ).

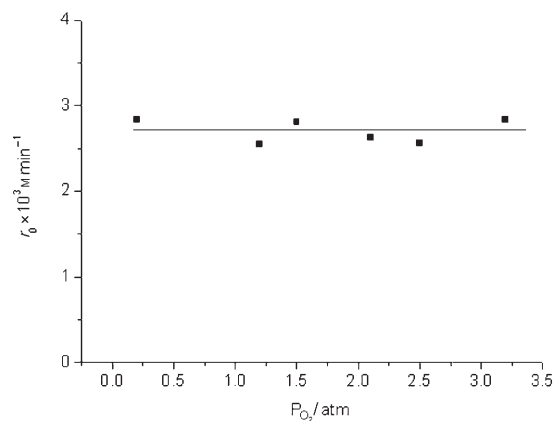


Figure 11. Initial reaction rate as a function of the oxygen pressure. Reaction conditions: benzyl alcohol (1 mmol), 0.44 wt% Au/npCeO<sub>2</sub> (0.2 mol%), toluene (5 mL), 90 °C,  $P_{O_2} = 0.2$ –3.2 atm. Slope =  $-1.6 \times 10^{-5}$ .

observed that  $r_0$  is independent of the oxygen pressure in the interval of pressures studied here. This zero order dependence of  $r_0$  versus oxygen pressure can be interpreted as an indication that the reoxidation of the metal hydride by molecular oxygen proceeds quickly and is not rate-controlling.

In another set of experiments, we studied the influence of the temperature on the reaction rate in the range from 60–90 °C for the aerobic oxidation *p*-methylbenzyl alcohol. By plotting  $\log r_0$  versus the inverse of the temperature, a good linear correlation was obtained from which the kinetic parameters, apparent activation energy ( $E_a$ ) and  $\log A$  could be estimated as 59.5 kJ mol<sup>-1</sup> and 22.4, respectively (Figure 12).

Additionally, the dependence of the reaction rate for the benzyl alcohol oxidation on the mol percentage of gold catalyst present in the reaction was investigated for the range between 0.05–0.2 mol% Au (Figure 13). In these experiments we used Au/npCeO<sub>2</sub> (0.45 wt% gold) and increas-

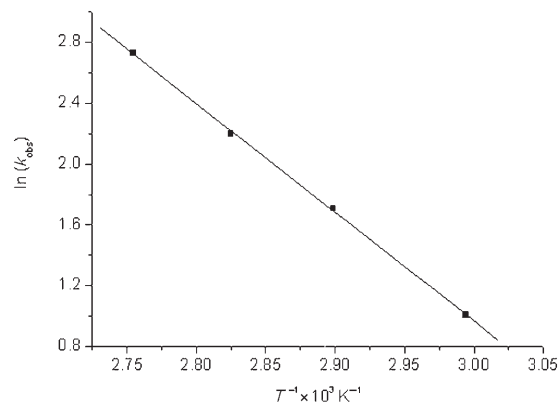


Figure 12. Arrhenius plots for the oxidation of *p*-methylbenzyl alcohol. The  $r_0$  values were regarded as the pseudo-zero-order rate constants ( $k_{obs}$ ) because the concentration of *p*-methylbenzaldehyde produced was proportional to time. Reaction conditions: *p*-methylbenzyl alcohol (1 mmol), 0.44 wt% Au/npCeO<sub>2</sub> (0.2 mol%), toluene (5 mL), 60–90 °C, atmospheric air as oxidant. Line Fit:  $\ln(k_{obs}) = 22.42 - 7150.96/T$  ( $r^2 = 0.99$ ).

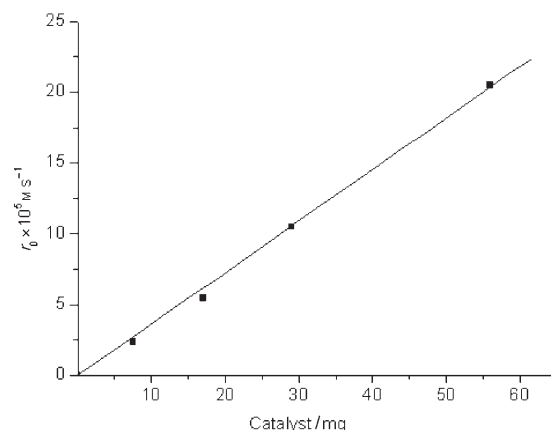


Figure 13. Effect of the amount of Au/npCeO<sub>2</sub> catalyst on the reaction rate oxidation of benzyl alcohol. Reaction conditions: benzyl alcohol (1 mmol), 0.44 wt% Au/npCeO<sub>2</sub> (0–54 mg), toluene (5 mL), 90 °C,  $O_2$  (air, 1 atm).

ing amounts of catalyst were added to the reaction system. The plot of the initial reaction rate versus the amount of gold in the system shows that the reaction rate follows a linear relationship with the gold content in the system, indicating a first order dependence between the concentration of gold in the reaction and the reaction rate.

The dependence of the reaction rate with the initial alcohol concentration for a given amount of Au/npCeO<sub>2</sub> catalyst at constant  $O_2$  pressure was established for the oxidation of 1 and 2-octanol. Figure 14 presents the plots of the initial reaction rate versus the alcohol concentration for the aerobic oxidation in toluene. For both alcohols it was observed that  $r_0$  increases with the initial alcohol concentration to reach a plateau corresponding to the maximum reaction rate. This behaviour is in accordance with a Langmuir–Hinselwood reaction mechanism (Scheme 4) and is in agreement with that



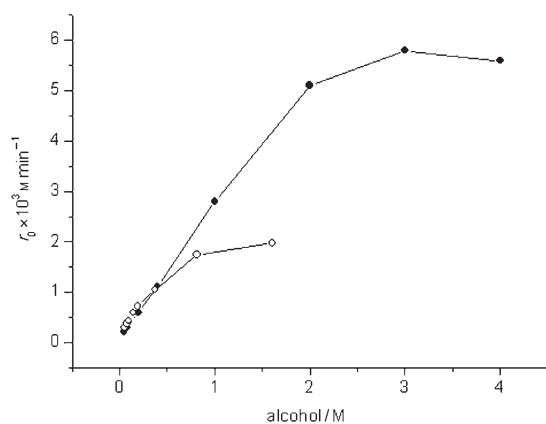
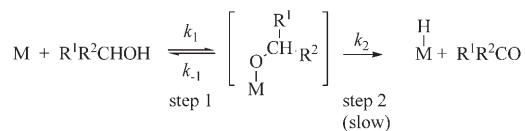


Figure 14. Effect of the concentration of alcohol in the reaction rate oxidation of 2-octanol (●) and 1-octanol (○). Reaction rates measured for conversions lower than 10%. Reaction conditions: [alcohol] (0.075–4 M in toluene), toluene (2.5 mL), 14 mg of 0.44 wt % Au/npCeO<sub>2</sub>, 90 °C.



Scheme 4. Simplified reaction mechanism for the aerobic oxidation of alcohols catalyzed by Au/npCeO<sub>2</sub>. R<sup>1</sup> = alkyl, aryl; R<sup>2</sup> = alkyl, aryl, H.

found by others for the aerobic oxidation of alcohols utilizing heterogeneous ruthenium catalysts.<sup>[46–47]</sup> According to this model, the free alcohol and the metal site would be in equilibrium with the M–alcoholate. Subsequently the M–alcoholate will react irreversibly to give rise to the reaction product and the M–hydride. The hydride shift from the alcohol to gold represents the rate-determining step.

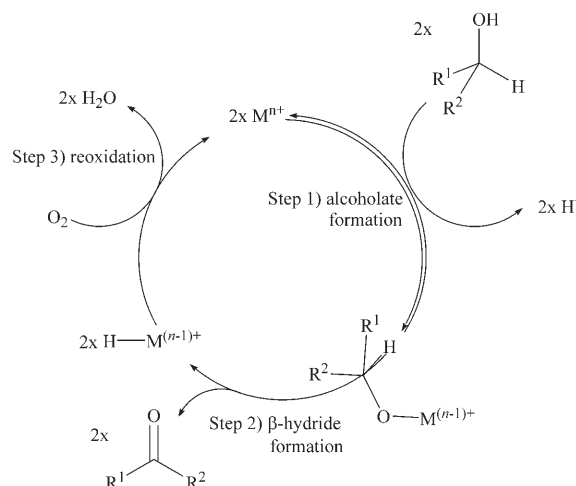
It can be observed (Figure 14) that the maximum rate for primary 1-octanol (although smaller than the maximum rate of secondary 2-octanol) is reached for alcohol concentration lower than for 2-octanol. In accordance with the Langmuir–Hinshelwood model the previous observation indicates that the binding constant of the metallic site for the primary alcohol is larger than for 2-octanol, because for the later secondary alcohol a larger excess is needed to reach the plateau. By using the Lineweaver–Burke formalism to plot the double inverse of the reaction rate and alcohol concentration,  $K_M$  and  $V_{\max}$  for 1- and 2-octanol were determined. These values can serve to understand the results of competitive primary versus secondary alcohol oxidation. Thus, even though the maximum reaction rate for 2-octanol is higher than for 1-octanol (see Table 3), when a mixture of the primary and secondary alcohols is submitted to oxidation, the primary alcohol is preferentially converted with respect to the secondary.

*Proposed reaction mechanism:* Based on the previous mechanistic and kinetic experiments for aerobic oxidation cata-

Table 3. Kinetic parameters in the aerobic oxidation of 1-octanol and 2-octanol by Au/npCeO<sub>2</sub> calculated by using Lineweaver–Burke plot.

	$K_m$ [M]	$V_{\max}$ [ $10^3 \text{ M min}^{-1}$ ]
1-octanol	0.344	2.07
2-octanol	1.209	5.72

lyzed by Au/npCeO<sub>2</sub>, reaction mechanism is presented in Scheme 5. According to this, the catalytic oxidation will go through three main reaction steps. The first one will be the



Scheme 5. The proposed mechanism for the Au/npCeO<sub>2</sub>-catalyzed aerobic oxidations of alcohols.

formation of M–alcoholate species that will be in equilibrium with the free alcohol. Under conditions in which a high concentration of alcohol is present a large majority of the metal sites will be coordinated forming the alcoholate.

This metal alcoholate species would undergo a metal–hydride shift giving rise to the carbonylic product and a metal–hydride intermediate. This step will be rate-determining, as it is deduced from the observation of a primary isotopic effect. The hydride shift and the metal–alcoholate bond breaking will be concerted events, but asynchronous. The hydride shift would progress in a larger extent than the metal alcoholate bond breaking. This proposal will be compatible with the moderate negative  $\rho$  value obtained for the different substituent in the *para*-position of the phenyl ring for the oxidation of benzyl alcohols. The third step will be the rapid oxidation of the metal hydride by oxygen to form water while recovering the initial metallic site. In this regard we point out that our previous in situ IR spectroscopy studies have shown that formation of the carbonyl compound occurs in a previous step and independent to the formation of water, while water is only formed when oxygen is admitted into the cell.<sup>[30]</sup> Also, gold-hydrides are known to be high in energy and very reactive.<sup>[48,49]</sup>

## Conclusion

From the results presented in this manuscript it is possible to say that the activity of gold catalyst for the aerobic oxidation of alcohols involves the presence of a high density of positive gold atoms that could act as Lewis-acid sites. These sites coordinate with alcohols to form gold alcoholates and they also accept hydrides. In this regard the role of the support should be on the one hand, to provide stability for positive gold species by interfacial gold-support interactions, and on the other hand to facilitate oxygen activation to promote the reoxidation of metal hydrides. Apparently these features and particularly the second one, have been achieved to a remarkable extent by cerium nanoparticles. Thus, cerium nanoparticles interact strongly with supported gold, as evidenced by the temperature of hydrogen reduction and also O<sub>2</sub> can be adsorbed through oxygen vacancies on the surface.<sup>[50]</sup> The combination of these properties explains the high and general activity of Au/npCeO<sub>2</sub> even in organic solvents, as we have shown here, and is in agreement with the reaction mechanism proposed.

## Experimental Section

### Preparation of Au/npCeO<sub>2</sub>

**Synthesis of nanoparticulated ceria:** The preparation of nanoparticulated ceria was carried out following a reported procedure.<sup>[51]</sup> In short, an aqueous solution of Ce(NO<sub>3</sub>)<sub>4</sub> (375 mL, 0.8 M) was treated, under stirring and at ambient temperature, with an aqueous solution of ammonia (1.12 L, 0.8 M). The colloidal dispersion of CeO<sub>2</sub> nanoparticles was heated in a PET vessel at 100 °C for 24 h. The resulting yellow precipitate was filtered and dried under vacuum overnight. The cerium oxide synthesised has, owing to the small size of the nanoparticles, a very high surface area (180 m<sup>2</sup> g<sup>-1</sup>).

Au was deposited on the nanoparticulated ceria by using the following procedure: A solution of HAuCl<sub>4</sub>·3H<sub>2</sub>O (800 mg) in deionised water (160 mL) was brought to pH 10 by addition of a solution of NaOH 0.2 M. Once the pH value was stable the solution was added to a gel containing colloidal CeO<sub>2</sub> (4.01 g) in H<sub>2</sub>O (50 mL). After adjusting the pH of the slurry at a value of 10 by addition of a 0.2 M solution of NaOH 0.2 M, the slurry was continuously stirred vigorously for 18 h at RT. The Au/npCeO<sub>2</sub> solid was then filtered and exhaustively washed with several litres of distilled water until no traces of chlorides were detected by the AgNO<sub>3</sub> test. The catalyst was dried under vacuum at room temperature for 1 h. Then 1-phenylethanol (30 g) was treated with the supported catalyst (3.5 g) at 160 °C and the mixture was allowed to react for 20 min. The catalyst was filtered, washed with acetone and water, and dried under vacuum at RT. The total Au content of the final catalyst Au/npCeO<sub>2</sub> was 4.5 wt % as determined by chemical analysis. For the preparation of 1.8 and 0.45 wt % Au/npCeO<sub>2</sub> the method used was the same as above, but changing only the amount of HAuCl<sub>4</sub>·3H<sub>2</sub>O aqueous. This catalyst Au/npCeO<sub>2</sub> is commercially available from Instituto de Tecnología Química (ITQ) (<http://www.upv.es/itq>).

**Preparation of 1 wt % Au/C catalyst:** A colloidal solution of gold nanoparticles stabilized by polyvinyl alcohol were deposited on activated carbon (KB-B-100, provided by Aldrich), following the procedure reported by Porta et al.<sup>[52]</sup> Under vigorous stirring an aqueous solution of HAuCl<sub>4</sub> (2 L, 100 µg mL<sup>-1</sup>) was treated with an aqueous solution of polyvinyl alcohol (PVA) (10 mL, 27 mg mL<sup>-1</sup>). To this, a fresh solution of NaBH<sub>4</sub> (38 mL, 0.1 M) was added. The AuNPs generated were immobilised simply by adding the active carbon (2 g) into the metal dispersion.

After 1 h the slurry was filtered and the total gold adsorption was checked by atomic absorption spectroscopy of the filtrate.

**Preparation of Au/TiO<sub>2</sub> catalysts:** The Au-TiO<sub>2</sub> catalysts were prepared by the deposition-precipitation method by using P-25 titanium oxide from Degussa as support. Particles of different sizes were obtained by changing the pH used in the deposition of gold nanoparticles over the TiO<sub>2</sub> support and the calcination temperature.

**Au-TiO<sub>2</sub> (5.2 nm mean diameter):** A solution of HAuCl<sub>4</sub>·3H<sub>2</sub>O (60 mg) in deionised water (30 mL) was brought to pH 6.3 by addition of a solution of NaOH (0.2 M). Once the pH value was stable, P-25 Degussa TiO<sub>2</sub> (1.0 g) was added. The slurry was vigorously stirred for 1 h at 70 °C. The Au/TiO<sub>2</sub> catalyst was then filtered and exhaustively washed with water. The catalyst was dried at 80 °C during 6 h and calcined using the following temperature program: room temperature, 3 °C min<sup>-1</sup>, 200 °C, 2 h. The total Au content of the final catalyst Au/TiO<sub>2</sub> was 2.9 wt % as determined by chemical analysis.

**Au-TiO<sub>2</sub> (7.3 nm mean diameter):** This Au-TiO<sub>2</sub> catalyst was prepared following the same procedure used in the synthesis of Au-TiO<sub>2</sub> (3.2 nm), but at pH value of 5.0 instead of 6.3. The dried solid was calcined at 400 °C during 2 h. The gold content of the final catalyst was 3.0 wt %.

**Au-TiO<sub>2</sub> (16.7 nm mean diameter):** The catalyst was prepared at pH 4.5 and calcined at 400 °C for 2 h. The gold content of the final catalyst was 2.8 wt %.

For crystal analysis and indexation, Au/npCeO<sub>2</sub> samples were examined by bright- and dark-field electron microscopy in a Jeol 2200 HRTEM (high-resolution transmission electron microscopy) operated at an accelerating voltage of 200 kV. The TEM images and the particle size distribution corresponding to Au/TiO<sub>2</sub> samples were obtained in a Philips-CM10 operated at 100 kV. Chemical analyses of gold in the catalysts were carried out after dissolving the solids by attack with a 2:1 mixture of HNO<sub>3</sub>/HF on a Varian-10 Plus Atomic Absorption Spectrometer or directly of the solids using a Philips Minipal 25 fm Analytic X-Ray apparatus and a calibration plot.

**Typical procedure for the aerobic oxidations of alcohols:** A suspension of 0.44 wt % Au/npCeO<sub>2</sub> (0.2 mol %) in toluene (5 mL) was treated with benzyl alcohol (1 mmol). The resulting mixture was then heated at 90 °C for 1 h and benzaldehyde was produced in > 99 % GC yield. After the reaction, the catalyst was separated by filtration and washed with acetone. The recovered Au/npCeO<sub>2</sub> was washed with an aqueous solution of NaOH (0.5 M) and water (100 mL) and dried under vacuum before recycling.

## Acknowledgement

Financial support by the Spanish DGI (CTQ06-6857) is gratefully acknowledged. A. A. thanks to the Spanish Ministry of Education for a postgraduate scholarship.

- [1] A. S. K. Hashmi, T. M. Frost, J. W. Bats, *J. Am. Chem. Soc.* **2000**, *122*, 11553.
- [2] A. S. K. Hashmi, M. C. Blanco, E. Kupejovic, W. Frey, J. W. Bats, *Adv. Synth. Catal.* **2006**, *348*, 709.
- [3] S. Carrettin, M. C. Blanco, A. Corma, A. S. K. Hashmi, *Adv. Synth. Catal.* **2006**, *348*, 1283.
- [4] C. González-Arellano, A. Abad, A. Corma, H. García, M. Iglesia, F. Sánchez, *Angew. Chem.* **2007**, *119*, 1558; *Angew. Chem. Int. Ed.* **2007**, *46*, 1536.
- [5] L. Zhang, S. A. Kozmin, *J. Am. Chem. Soc.* **2004**, *126*, 11806.
- [6] L. Zhang, S. A. Kozmin, *J. Am. Chem. Soc.* **2005**, *127*, 6962.
- [7] R. O. C. Norman, W. J. E. Parr, C. B. Thomas, *J. Chem. Soc. Perkin Trans. I* **1976**, 811.
- [8] A. S. K. Hashmi, L. Schwarz, J. H. Choi, T. M. Frost, *Angew. Chem.* **2000**, *112*, 2382; *Angew. Chem. Int. Ed.* **2000**, *39*, 2285.
- [9] C. G. Yang, C. He, *J. Am. Chem. Soc.* **2005**, *127*, 6966.
- [10] J. Zhang, C. G. Yang, C. He, *J. Am. Chem. Soc.* **2006**, *128*, 1798.

- [11] R. V. Nguyen, Z. Yao, C. J. Li, *Org. Lett.* **2006**, *8*, 2397.  
 [12] X. Zhang, A. Corma, *Chem. Commun.* **2007**, 3080.  
 [13] G. C. Bond, P. A. Sermon, G. Webb, D. A. Buchanan, P. B. Wells, *J. Chem. Soc. Chem. Commun.* **1973**, *13*, 444b.  
 [14] P. A. Sermon, G. C. Bond, P. B. Wells, *J. Chem. Soc. Faraday Trans. 1* **1979**, 385.  
 [15] J. E. Bailie, G. J. Hutchings, *Chem. Commun.* **1999**, 2151.  
 [16] P. Claus, *Appl. Catal. A* **2005**, *291*, 222.  
 [17] P. Concepción, P. Serna, A. Corma, *Angew. Chem.* **2007**, *119*, 7404; *Angew. Chem. Int. Ed.* **2007**, *46*, 7266.  
 [18] A. Corma, P. Serna, H. García, *J. Am. Chem. Soc.* **2007**, *129*, 6358.  
 [19] M. Haruta, T. Kobayashi, H. Sano, N. Yamada, *Chem. Lett.* **1987**, *16*, 405.  
 [20] G. C. Bond, D. T. Thompson, *Gold Bull.* **2000**, *35*, 41.  
 [21] M. Haruta, *Nature* **2005**, 437.  
 [22] L. Prati, M. Rossi, *J. Catal.* **1998**, *176*, 552.  
 [23] S. Carrettin, P. McMorn, P. Johnston, K. Griffin, G. J. Hutchings, *Chem. Commun.* **2002**, *7*, 696.  
 [24] A. Corma, M. Domine, *Chem. Commun.* **2005**, *32*, 4042.  
 [25] A. S. K. Hashmi, G. J. Hutchings, *Angew. Chem.* **2006**, *118*, 8064; *Angew. Chem. Int. Ed.* **2006**, *45*, 7896.  
 [26] M. Comotti, C. D. Pina, R. Matarrese, M. Rossi, *Angew. Chem.* **2004**, *116*, 5936; *Angew. Chem. Int. Ed.* **2004**, *43*, 5812.  
 [27] A. Abad, P. Concepción, A. Corma, H. Garcia, *Angew. Chem.* **2005**, *117*, 4134; *Angew. Chem. Int. Ed.* **2005**, *44*, 4066; .  
 [28] K. Mori, T. Hara, T. Mizugaki, K. Ebitani, K. Kaneda, *J. Am. Chem. Soc.* **2004**, *126*, 10657.  
 [29] D. I. Enache, J. K. Edwards, P. Landon, B. Solsona-Espriu, A. F. Carley, A. A. Herzing, M. Watanabe, C. J. Kiely, D. W. Knight, G. J. Hutchings, *Science* **2006**, *311*, 362.  
 [30] A. Abad, C. Almela, H. Garcia, A. Corma, *Tetrahedron* **2006**, *62*, 6666.  
 [31] A. Abad, C. Almela, H. Garcia, A. Corma, *Chem. Commun.* **2006**, 3178.  
 [32] M. Haruta, *Catal. Today* **1997**, *36*, 153.  
 [33] L. Prati, M. Rossi, *Stud. Surf. Sci. Catal.* **1997**, *110*, 509.  
 [34] M. Haruta, N. Yamada, T. Kobayashi, S. Iijima, *J. Catal.* **1989**, *115*, 301.  
 [35] B. S. Uphade, Y. Yamada, T. Akita, T. Nakamura, M. Haruta, *Appl. Catal. A* **2001**, *215*, 137.  
 [36] G. C. Bond, D. T. Thompson, *Catal. Rev.-Sci. Eng.* **1999**, *41*, 319.  
 [37] G. C. Bond, D. T. Thompson, *Gold Bulletin* **2000**, *33*, 41.  
 [38] R. Van Hardeveld, F. Hartog, *Surf. Sci.* **1969**, *15*, 189.  
 [39] R. E. Benfield, *J. Chem. Soc. Faraday Trans.* **1992**, *88*, 1107.  
 [40] F. Esch, S. Fabris, L. Zhou, L. Montini, C. Africh, P. Fornasiero, G. Comelli, R. Rosie, *Science* **2005**, *309*, 752.  
 [41] M. Valden, X. Lai, D.W Goodman, *Science* **1998**, *281*, 1647.  
 [42] T. Mallat, A. Baiker, *Chem. Rev.* **2004**, *104*, 3037.  
 [43] P. Migowski, J. Dupont, *Chem.-A Eur. J.* **2006**, *13*, 32.  
 [44] D. Astruc, L. Fung, J. Aranzaes, *Angew. Chem.* **2005**, *117*, 4134; *Angew. Chem. Int. Ed.* **2005**, *44*, 7852.  
 [45] J. Dupont, G. S. Fonseca, A. P. Umpierre, P. F. P. Fichtner, S. R. Teixeira, *J. Am. Chem. Soc.* **2003**, *124*, 4228.  
 [46] K. Yamaguchi, N. Mizuno, *Chem.-Eur. J.* **2003**, *9*, 4353.  
 [47] K. Ebitani, K. Motokura, T. Mizugaki, K. Kaneda, *Angew. Chem.* **2005**, *117*, 3489; *Angew. Chem. Int. Ed.* **2005**, *44*, 3423.  
 [48] P. Schwerdtfeger, P. D. W. Boyd, S. Brienne, A. K. Burrell, *Inorg. Chem.* **1992**, *31*, 3411.  
 [49] X. F. Wang, L. Andrews, *Angew. Chem.* **2003**, *115*, 5359; *Angew. Chem. Int. Ed.* **2003**, *42*, 5201.  
 [50] V. V. Pushkarev, V. I. Kovalchuk, J. L. D'Itri, *J. Phys. Chem. B* **2004**, *108*, 5341.  
 [51] J. Y. Chane-Ching (Rhône Poulenc Spec Chim, France), EP0208580, **1987**.  
 [52] F. Porta, L. Prati, M. Rossi, S. Coluccia, G. Martra, *Catal. Today* **2000**, *61*, 165.

Received: August 14, 2007

Revised: October 8, 2007

Published online: November 23, 2007